

Revealing the mechanism for rapid growth of organic-inorganic halide perovskite crystals

Pabitra K. Nayak^{1a}, David T. Moore^{1,2a}, Bernard Wenger¹, Simantini Nayak³, Amir A. Haghighirad¹, Adam Fineberg⁴, Nakita K. Noel¹, Obadiah G. Reid², Garry Rumbles,² Philipp Kukura⁴, Kylie A. Vincent³, Henry J. Snaith^{1*}

¹Clarendon Laboratory, University of Oxford, Parks Road, Oxford, OX1 3PU, UK

²National Renewable Energy Lab, Golden, CO 80401, USA

³Department of Chemistry, University of Oxford, Inorganic Chemistry Laboratory, South Parks Road, Oxford, OX1 3QR, UK

⁴Physical and Theoretical Chemistry Laboratory, University of Oxford, South Parks Road, Oxford, OX1 3QZ, UK

^a Equal contribution

E-mail: henry.snaith@physics.ox.ac.uk

Abstract: Photovoltaic devices based on organic-inorganic halide perovskites have shown remarkably rapid progress to high efficiency, and now alternative optoelectronic devices, such as light emitting diodes and photodetectors, are also exhibiting competitive performance. However, despite their phenomenal performances in devices, there remain many open questions with regards to the basic properties of this type of material. Use of single crystals is often seen as the ideal platform for understanding the limits and possibilities associated with a material. Macroscopic perovskite crystals have recently been realised by a rapid, facile crystallisation route where the crystals are produced by increasing the temperature of the solution. However, there is little known regarding the mechanism of this type of crystal growth. A proper understanding of the mechanism will enable a critically needed advance in the reproducibility and quality of single crystals for fundamental studies as well as applications in single-crystal optoelectronic devices. Here we find that the observed rapid crystallisation of metal halide perovskite crystals at higher temperatures is due to reversible changes in the colloidal solutions where breaking up of colloids and a change in the solvent strength lead to the supersaturation

of solutes and subsequent crystallization. Now, with the new knowledge regarding the mechanism, we have demonstrated that a much broader range of parameters including the temperature range and solvent/salt combinations can be used to produce various types of perovskite single crystals. We also show that the quality of the single crystals can be improved by reducing the temperature of crystallisation. Our findings are therefore of central importance to enabling the continued advancement of perovskite optoelectronics and to the improved reproducibility through better understanding of factors influencing and controlling crystallisation.

Organic-inorganic halide perovskite semiconductors, archetypically $\text{CH}_3\text{NH}_3\text{PbX}_3$ ($\text{X}=\text{Cl}, \text{Br}$ or I), have attracted significant attention due to their remarkable performance in optoelectronic devices.¹⁻³ A key driving factor to the optoelectronic performance is the low energy of crystal formation and the relative ease with which highly crystalline films of high electronic quality can be produced.⁴⁻⁶ In spite of this ease of processing and remarkable performance, there remain many open questions with regards to the fundamental, intrinsic properties of this class of materials. For a crystalline material, the use of single crystals is frequently seen as the ideal platform for discerning these intrinsic properties. However, the processing pathways typically used for single crystals suffer from low throughput which hinders their study on a broad scale. Macroscopic perovskite crystals have recently been realised by a rapid, facile crystallisation route which has been attributed to an “inverse solubility” effect.⁷⁻⁹ In addition to delivering high quality crystals,¹⁰ the nature of the rapid crystallisation is closely related to the crystallisation of perovskites in thin films,¹¹ and proper understanding of the mechanism will enable a critically needed advance in the reproducibility and quality of both thin films and single crystals for optoelectronic devices.

In this work, we show that the crystallisation in solution is initiated by an in-situ change in the solvent composition, specifically a change in acid-base equilibrium which raises the concentration of solute species, due to the dissolution of colloids, resulting in supersaturation. With this knowledge we establish the rapid crystallisation of macroscopic perovskite crystals across a wider range of concentrations, temperatures and solvents than previously reported and reveal how this broader parameter space can produce crystals of comparatively enhanced optoelectronic quality by enabling crystallization at lower temperatures.

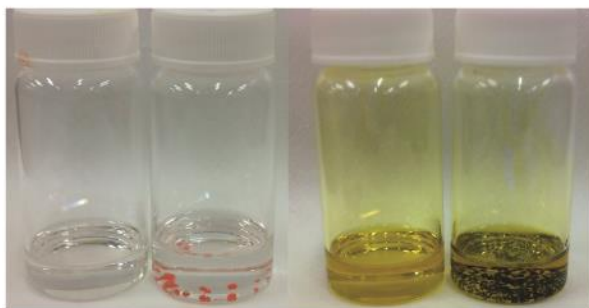
The driving force for crystallisation from solution is supersaturation, therefore, determining the cause of crystallisation is synonymous with determining the mechanism by which a solution reaches its solubility limit. Typically, to define solubility, the saturation concentration is presented as a function of temperature. Inverse solubility, which is still presented as the temperature dependence of the saturation point, exists when the saturation concentration decreases with increasing temperature.

Solubility, normal or inverse, is a thermodynamic consideration and, as such, a given salt-solvent system at a given concentration should reach saturation at the same temperature, and in the same amount of time. However, we find that the time and temperature required for crystallisation of metal halide perovskites varies depending on the age of the solvent (dimethylformamide (DMF) or γ -butyrolactone (GBL)). Additionally, significantly different saturation concentrations have been reported for the same salt-solvent combinations at the same temperature.^{7,9,12} These observations point toward a different mechanism, beyond simple ionic solubility consideration, by which saturation is reached.

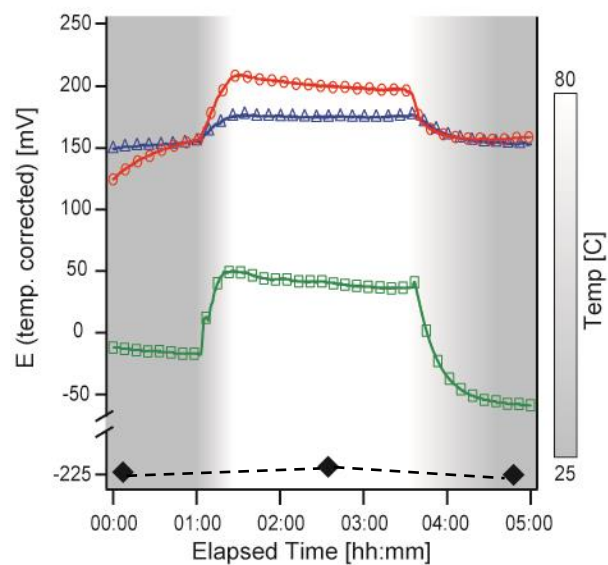
We begin our investigation by looking at the solvent and how its composition may change in the current system. The reported routes to grow $\text{CH}_3\text{NH}_3\text{PbBr}_3$ or $\text{CH}_3\text{NH}_3\text{PbI}_3$ single crystals have predominantly involved the dissolution of the reagent salts in DMF or GBL respectively, with a subsequent rise in temperature until crystallisation occurs.⁷⁻⁹ Because the solvents used were specific,

the same for all reports, and in all but one report exclude dimethylsulfoxide (DMSO), we reviewed the typical decomposition products for DMF, GBL, and DMSO. DMF can decompose into formic acid (FAH) and dimethylamine (DMA) and GBL can decompose to γ -hydroxybutyric acid (GHB);^{13,14} in contrast, DMSO produces no acidic component upon decomposition. To determine if this change in solvent composition (and acidity), independent of temperature, could induce the spontaneous crystallisation of organic-inorganic halide perovskites, we test the crystallisation in both DMF, with the addition of FAH, and GBL, with the addition of GHB (the decomposition products). We begin by replicating the systems as previously reported, a 1M solution of bromide salts ($\text{CH}_3\text{NH}_3\text{Br}$ and PbBr_2) in DMF and iodide salts ($\text{CH}_3\text{NH}_3\text{I}$ and PbI_2) in GBL, but with temperatures $\sim 25\text{--}30^\circ\text{C}$ lower than those required to induce crystallisation in the prior report.⁷ Under these conditions we do not observe any crystallization, even after several hours of heating. We then add FAH to the DMF and GHB to the GBL and we observe that crystallisation begins within 5 minutes. In Figure 1a we show an image of the crystals in solution alongside the control vials into which no acid was added. Since DMSO has no acidic byproduct, we can verify if acidity alone can cause supersaturation by attempting to crystallize the chloride system in DMSO by addition of FAH.¹⁵ We observe that a concentrated solution of the chloride salts ($\text{CH}_3\text{NH}_3\text{Cl}$ and PbCl_2 at 2M concentration) does not precipitate crystals when incubated at elevated temperatures (up to 80°C) for several hours. However, on addition of FAH (3 vol% with respect to the initial solution), we observe crystals of $\text{CH}_3\text{NH}_3\text{PbCl}_3$ being formed within 5 minutes at 70°C , indicating the effect is initiated by a change in the solvent composition and not directly related to temperature. We note that Liu, et al, have reported crystallisation of $\text{CH}_3\text{NH}_3\text{PbCl}_3$ from DMSO at 2M and 100°C . We are unable to reproduce their results without the addition of FAH, but highlight this as an ambiguity.⁹ We show photographs, absorption spectra (Extended Data, Fig. S2 and S3) and X-ray diffraction data (Extended Data Table S1) of $\text{CH}_3\text{NH}_3\text{PbCl}_3$, $\text{CH}_3\text{NH}_3\text{PbBr}_3$ and $\text{CH}_3\text{NH}_3\text{PbI}_3$ single crystals in the extended data to confirm the materials and their crystallinity.

(a)



(b)



(c)

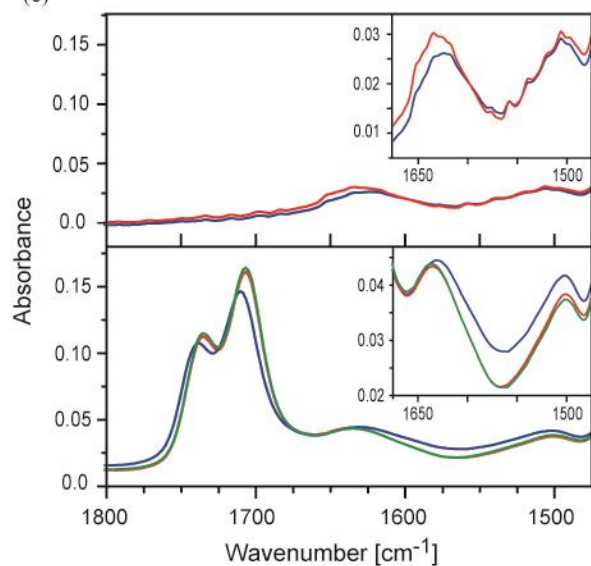
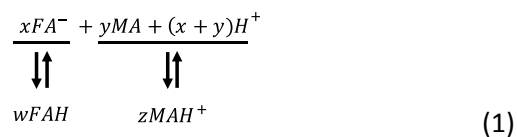


Figure 1: a) Photograph of the acid initiated crystallization for the bromide (clear solution) and iodide (yellow solution) systems; the vials with no crystals were kept for 24 hours at the crystallization temperature with no added acid, the vial with crystals had acid added ~2 hours prior to the picture being taken. b) potential measurements for DMSO; neat (black diamonds, see Extended Data for measurement details of neat DMSO), with 1M chloride salts

(green, squares), with 3 vol% FAH (red, circles), and with 1M iodide salts and 3 vol% FAH (blue, triangles), temperature indicated by the background gradient with the scale bar to the right. (c) In-situ FTIR data of 1.5M solution of chloride salts in DMSO with no FAH added (top) and with FAH added (bottom); data is taken initially at 25 °C (red), at 55 °C (blue), then again after cooling back to 25 °C (green). Insets are expanded to show the MA/MAH⁺ peaks between 1500 and 1650 cm⁻¹.

In previous reports the crystallization was reversible, i.e. when the temperature was decreased, crystals were dissolved; although the addition of an acid isn't reversible (nor is the in situ production of acid from the solvent due to solvent degradation) the change in acidity (protonation or deprotonation of the acid) can be reversed. To verify that this change in acidity can occur, we perform electrochemical experiments and record the potential change of a pH specific electrode as a function of temperature for a variety of systems. We utilize DMSO, due to its lack of acid byproduct, to test solutions with the reagent salts only, with 3 vol% added formic acid only, and with both the salts and the formic acid (we performed similar test for DMF, GBL and the neat solvents and show details in the Extended Data). We show the key results in Fig. 1b; for all solvents the addition of only the reagent salts (CH₃NH₃X + PbX₂) results in an increase in proton activity prior to any heating. Given that the only acid component in the DMSO solution is CH₃NH₃⁺ (MAH⁺), this must be due to the deprotonation of MAH⁺ to methylamine (MA) and H⁺. Additionally, for all solvents with both salts and added acid, the acidity is not additive for the salts and acid alone, which points to a shift in the acid/base equilibria as we depict below:



where w, x, y, and z are undetermined stoichiometric coefficients. It is also clear that, when all components are present, the change in acidity is reversible. We note that this data infers that the

change to the solvent with increasing and reducing temperature is not the production of additional acid by solvent degradation, but a shift in the equilibria in Eqn. 1.

To determine which species are changing, we perform in-situ attenuated total reflection infrared (ATR-IR) spectroscopy of solutions at different temperatures (see Extended Data for experimental details and extended discussion). There are two peaks of interest for both of the acids present, for FAH they are at $\sim 1700 - 1750 \text{ cm}^{-1}$ and for MAH^+ at ~ 1500 and 1625 cm^{-1} ; for both acids the absorbance should decrease as the acid is deprotonated.^{16,17} In Fig. 1c we show the IR absorption spectrum of $1.5 \text{ M MA} \cdot \text{Cl}_2 + \text{PbCl}_2$ in DMSO initially at 25°C , at 55°C , and again at 25°C after cooling. In the top plot of Fig. 1c we show the result with no FAH added: We observe a slight decrease in the absorbance, consistent with the deprotonation of MAH^+ at elevated temperature, which correlates with the electrochemical results. In the bottom plot of Fig. 1c we show the result when FAH is included: Here we observe that in the presence of both acids, the increase in temperature causes the deprotonation of FAH (absorbance decreases) and the protonation of MA (absorbance increases); we observe that when we cool, the effect is reversible. We interpret these ATR-IR results to indicate that the heating of a solution of the reagent salts in a solvent that includes a weak carboxylic acid pushes the MA/MAH^+ equilibrium in equation 1 towards increasing MAH^+ .

The combination of the electrochemical and ATR-IR results allows us to determine that the solvent, which we typically take to be, for example, DMF, is more accurately described as $\text{DMF} + \text{FAH} + \text{MA}$; where the FAH can come from the natural decomposition of DMF or from direct addition. The change in the solvent that influences the supersaturation concentration of reagent salts is when FAH deprotonates causing a reduction in MA; this change in FAH can be affected by raising the temperature, but it can also be initiated by adding FAH isothermally.

Determination of the changes to the solvent, specifically the existence and change in concentration of MA, prompts us to consider the role MA plays in solvation. Previous reports have shown a strong solvent annealing effect with MA vapour and that a solution of $\text{CH}_3\text{NH}_3\text{PbI}_3$ can be made in MA at 85 wt%.¹⁸ When we bubble MA into a vial containing $\text{CH}_3\text{NH}_3\text{PbBr}_3$ crystals, in equilibrium with a saturated solution of the bromide salts, the crystals dissolve implying that the MA/solvent mixture acts as a stronger solvent than the neat solvent alone (See Extended Data for details). The summary of our experiments exploring the solvent is that it changes by a change in acidity and that the solvent becomes weaker as the acidity is increased.

We next use our knowledge of the solvent changes to consider how it affects the solutes. Previous work has shown that these solutions consist not only of solvated ions, but also contain lead halide colloids and complexes. To determine whether the colloids impact the crystal formation, we remove some fraction of the colloids by centrifuging the salt solutions where we expect the solvated ionic species to remain in the solution due to their smaller size. We see that removing the colloids dramatically changes the onset temperature of crystallisation as well as the yield (see Extended data). This indicates that the ions which are incorporated in the colloids at room temperature, are important for and involved in some manner in the perovskite crystallisation. If the colloids dissolve with increasing temperature, then this could be the source of ions which lead to supersaturation. In order to assess if increasing temperature alone can result in dissolution of the colloids we perform static light scattering (SLS) experiments as a function of temperature; generally, a decrease in the scattering intensity denotes a decrease in the mean colloid particle size and/or particle concentration (see Extended Data for experimental details). We present results for a solution of 2M chloride salts in DMSO (no acidic degradation product from the solvent, the only acid present is MAH^+) in figure 2a, and we observe a negligible change in scattering intensity with increasing temperature. This indicates that temperature, and the small resulting change in acidity shown in Fig. 1b, has a negligible influence upon the colloids in

this system. Upon the addition of FAH (2.5 vol%) to the 2M chloride salts in DMSO, we observe a monotonic decrease of the light-scattering intensity as the solution is heated. This decrease in scattering intensity continues until $\sim 75^{\circ}\text{C}$ where we see a sharp rise in scattering intensity. Visual inspection at this temperature reveals that this inflection coincides with the formation of perovskite crystals. This is a clear indication that an increase in acidity can cause dissolution of colloids and subsequent rapid crystallisation of perovskites. In figure 2b, we show light scattering data for the bromide salts in DMF, where we also observe a decrease in scattering intensity as the temperature is increased, even without added FAH. For this system, this may be due to some small amount of FAH being present in “fresh” DMF or a stronger deprotonation of MAH^+ than in DMSO, or the colloids are more labile in this system. However, with increasing concentration of FAH in the bromide salts in DMF solution, we observe the light-scattering intensity drop further, and the onset temperature for crystallisation (as indicated by inflection of the scattering) drops monotonically to lower temperatures. We observe similar results for the iodide salts in GBL (Figs. S10). To summarise this section, the light scattering results are consistent with the colloids being increasingly dissolved or broken up with increasing acidity (where the acidity is a function of temperature), until the point at which supersaturation is reached, and the crystallisation proceeds. We also note that we observe an increase in the light scattering intensity upon lowering the temperature, which finally returns to the initial value, which is consistent with the dissolution of and formation of colloids being reversible. We associate this reversible dissolution to the reversibility of proton activity in the solution which in turn depends on the temperature of the system.

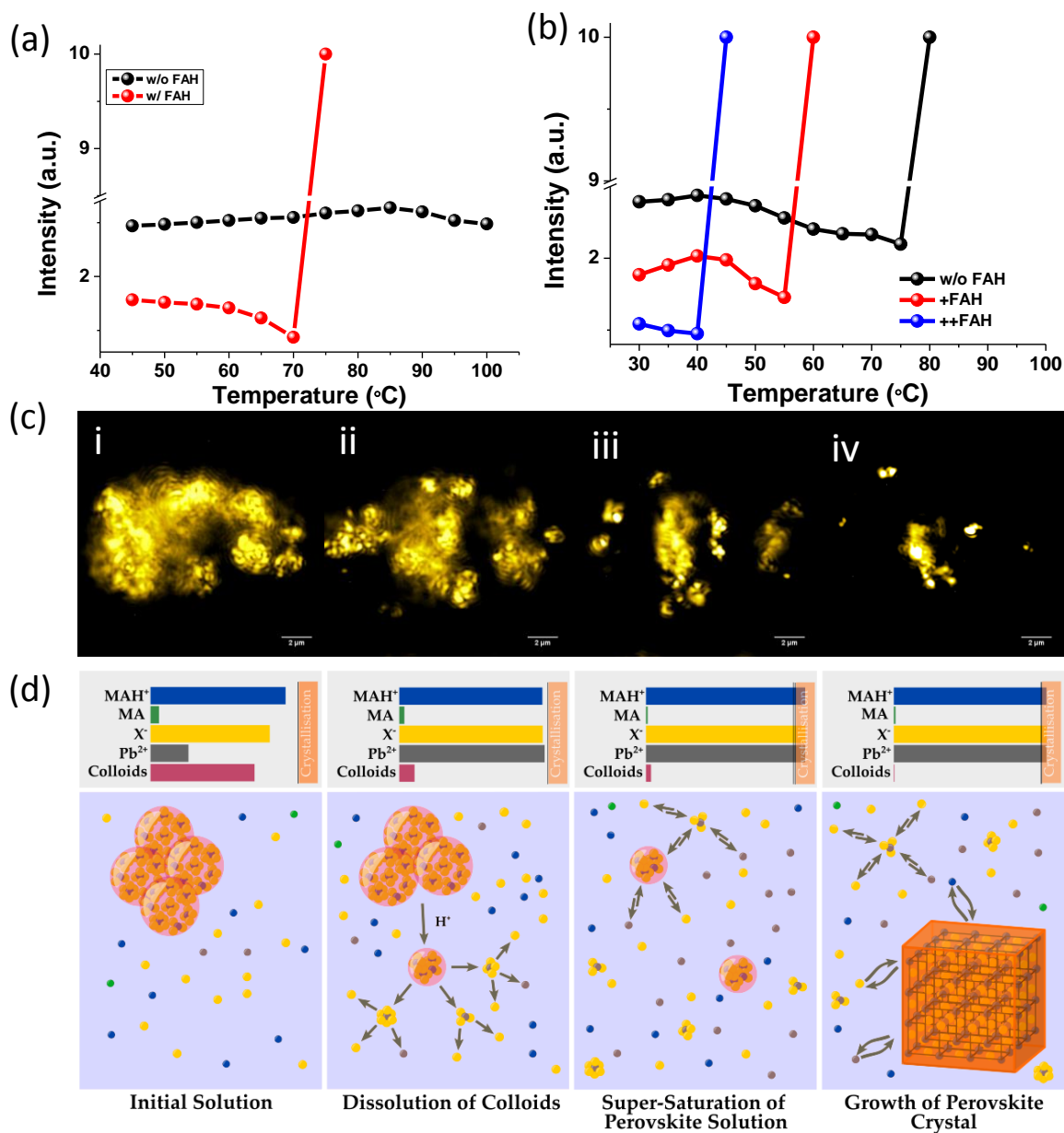


Figure 2: (a) Effect of added acid and temperature on the scattered light intensity of MAI+PbCl₂ in DMSO. (b) Effect of added acid and temperature on scattered light intensity of MABr+PbBr₂ in DMF. In both the graphs, the value of 10 (a.u.) represents the saturation point of the detector. (c) Micrographs from iSCAT imaging of dissolution of colloids after addition of FAH (10 vol%) in the 1 M MAI + PbI₂ in GBL at room temperature (movie file is available online). (d) Schematic representation of the crystallisation mechanism; horizontal bars on the top of each panel represent the concentration Pb²⁺, X⁻, MAH⁺, MA and colloids (not to scale) and spheres with similar colour schematically represents each species in the bottom panel. The vertical bar in the top panel represents the regime for crystallization (i.e. supersaturation).

In order to confirm and visualise the dissolution of the colloids, we employ interferometric scattering microscopy (iSCAT), and show micrographs of time sequence of the iodide salts dissolved in GBL following addition of FAH in Fig. 2c (the full movie file is available online). We observe the colloids breaking up and dissolving with the addition of FAH, even at a fixed temperature, confirming our interpretations from the static light scattering. We show the iSCAT images as a function of increasing temperature in Fig. S11 and confirm that the decrease in intensity in the light-scattering data corresponds to a disintegration of aggregated colloids followed by dissolution of the colloids. Importantly, during these measurements, we captured images of crystallisation occurring. In figure S12 we show a sequence of events during MAPbBr_3 crystal formation where we see that the crystals are growing from *clear solution* rather than from detectable colloids. This indicates that the visible colloids are an important source of free ions, but are not directly partaking in crystal growth. In summary of our examination of the solute, the colloids are in equilibrium with solvated ionic species and an increase in acidity dissolves the colloids in solution, leading to an increased concentration of dissociated ions.

Our examination of both the solvent and the solutes shows that both are changing as the acidity of the solution is increased. Further, we show that this increase in acidity can be initiated by the direct addition of acid, and although a change in temperature will also increase the acidity, it is not a necessary condition. From our solvent examination we know that an increase in acidity lowers the strength of the solvent by protonating MA and removing it from the solvent (MAH^+ is a solute). From our solute studies we know that the increase in acidity dissolves the lead halide colloids. This allows us to hypothesize the mechanism for crystallisation which we visualize in figure 2d where we schematically represent the state of the system at several key points. In its initial state, the solution is depleted in all the components i.e. the Pb^{2+} and halide ions contained in colloids, and the MAH^+ due to partial deprotonation. When proton

activity increases, by deliberate addition to the system or by dissociation of existing acid with increasing temperatures, three changes occur: (a) lead halide colloids are dissolved and produce a higher concentration of the ion species required for crystal formation, (b) the concentration of MAH^+ is increased due to protonation of the MA, and (c) the solvent becomes weaker due to a lower concentration of the MA. In other words, an increase in acidity raises the concentration of all solutes, while simultaneously decreasing the strength of the solvent; this results in supersaturation and the onset of crystallisation. We tested our hypothesis through a variety of controls including shifting the acid/base equilibria via addition of different bases and isothermal crystallisation of all systems discussed; we give details and discussion of these controls in the Extended Data. We note that we can also crystallize the caesium system (CsPbBr_3) by addition of acid to a DMSO solution (details in the Extended Data); although this doesn't discount the change in solvent strength in those systems where MAH^+ exists, it does infer that the effect of dissolving the colloids can be sufficient by itself to induce supersaturation and crystallisation.

During revisions of this manuscript there has been a report of crystallisation of MAPbCl_3 using DMSO, but with the addition of chlorobenzene (CB) to the solution, which is an "anti-solvent" for the perovskite.¹⁹ This report indicates that the addition of an "anti-solvent" is also capable of initiating crystallisation, and reducing the onset temperature. This raises the question as to whether the anti-solvent is simply reducing the solvent strength, or also influencing the dissolution of colloids, whether directly, or through an indirect influence upon the acid-base equilibrium of the solution. In addition, it raises the question as to whether or not FAH is simply acting as an anti-solvent. In order to confirm that FAH is not simply an anti-solvent, we attempted to dissolve MAPbI_3 perovskite crystals in FAH and CB selectively. While for CB we observe the perovskite crystals remain undissolved, for FAH, they dissolve into a turbid solution (see Extended Data). This indicates that FAH is not a typical anti-solvent. There clearly remain open questions as to the relationship between our observed acid induced crystallization

and the anti-solvent induced crystallization. Specifically, a deeper level of knowledge is still required to understand what fundamentally drives the dissolution of colloids, which shifts the concentration of free-ions into the supersaturated regime. Understanding these further aspects is the focus of ongoing research in our groups.

It is commonly understood that single crystals of semiconducting materials ultimately have improved properties over polycrystalline thin films due to the elimination of grain boundaries and compositional inhomogeneity. Hence, the understanding of single crystal growth we have delivered here will have a significant impact upon the community advancing single crystal perovskites for optoelectronics. Here we demonstrate three accomplishments enabled by this deeper knowledge: (1) crystallisation of additional salt/solvent combinations (see Extended data), (2) an increased yield (see extended data), and (3) preparation of crystals of all three salts over a wider range of temperatures, ranging from 50-80 °C for the chloride, 30-100 °C for the bromide, and 48-120 °C for the iodide systems. In figure S2 we show the optical images of cm scale crystals of $\text{CH}_3\text{NH}_3\text{PbCl}_3$, $\text{CH}_3\text{NH}_3\text{PbBr}_3$ and $\text{CH}_3\text{NH}_3\text{PbI}_3$ all grown at 55 °C. Further, we demonstrate the impact of this broadened set of processing parameters by growing iodide crystals below the tetragonal-cubic phase transition temperature.

We can now grow $\text{CH}_3\text{NH}_3\text{PbI}_3$ crystals at temperatures ranging from 48-100 °C, and we characterise them by single crystal diffraction and optical measurements. We perform single crystal diffraction on three crystals grown at 55, 70 and 100 °C, and show the full data set in the Extended Data. As the growth temperature decreases we observe an improvement in the overall fit parameters, less twinning, and an increased tilt between adjacent lead halide octahedra (See Table S4 and Fig. S19), indicating that controlling the temperature of growth, has a structural impact upon the final crystal.

We next explore the impact of the temperature of crystallization upon the optical properties of crystals.

We show time-resolved photoluminescence (TRPL), using both 1-photon (1P) and 2-photon (2P)

excitation, on crystals grown at 48 °C (below the tetragonal to cubic phase transition) and 95 °C in Fig. 3a (2P) and Fig. S20 (1P). Photoluminescence in lead-halide perovskites originates from band-to-band recombination of free electrons and holes.²⁰ The 2nd order recombination rate scales as the product of the electron and hole number density. But at low excitation fluences, the lead-halide perovskites exhibit a 1st order recombination rate, governed by trap assisted recombination. For 1P excitation (2.33 eV), the incident light of above band gap energy (~ 1.55 eV) is absorbed strongly in the crystal within a penetration depth of ~ 170 nm. Hence most of the free charges are generated near the surface of the crystal. For 2P excitation, the sub-band gap photon energy (0.89 eV) has very low absorbance; owing to this the light absorption, and charge generation, is distributed over the entire thickness of the crystal. As a result, the 2P measurements probe a substantially larger bulk volume than surface volume, and the 2P PL data contains more information about the bulk properties.²¹ For both 1P and 2P PL, the initial decay is dominated by a fast process, followed by a slower, exponentially decaying component. We quantify the slow 1st order decay rates by fitting the slowest part of the decays measured at various excitation fluences with a single exponential (see details in Extended Data). With 1-photon excitation, the first order decay coefficient, k_1 , is equivalent for crystals grown at different temperatures. We note that the estimated k_1 is very similar to high quality polycrystalline perovskite films used in photovoltaic devices ($k_1 \sim 5 \cdot 10^6 \text{ s}^{-1}$).²⁰ This implies that the surface region of single crystals is similar to polycrystalline thin films in terms of recombination site density. As we expect, the 2P measurements reveal longer PL lifetimes for both crystals, with k_1 reduced by one order of magnitude, in agreement with the values found by Yamada et. al.²¹ Because of these long lifetimes we can infer that the bulk defect density in single crystals is lower than at the surface. When the crystal is grown at 48 °C the recombination is further decreased by a factor of 2 with respect to the 95 °C grown crystal. Thus, our measurements are consistent with the crystal grown at lower temperature having a lower non-radiative recombination site density in the bulk of the crystal, and hence improved optoelectronic quality.

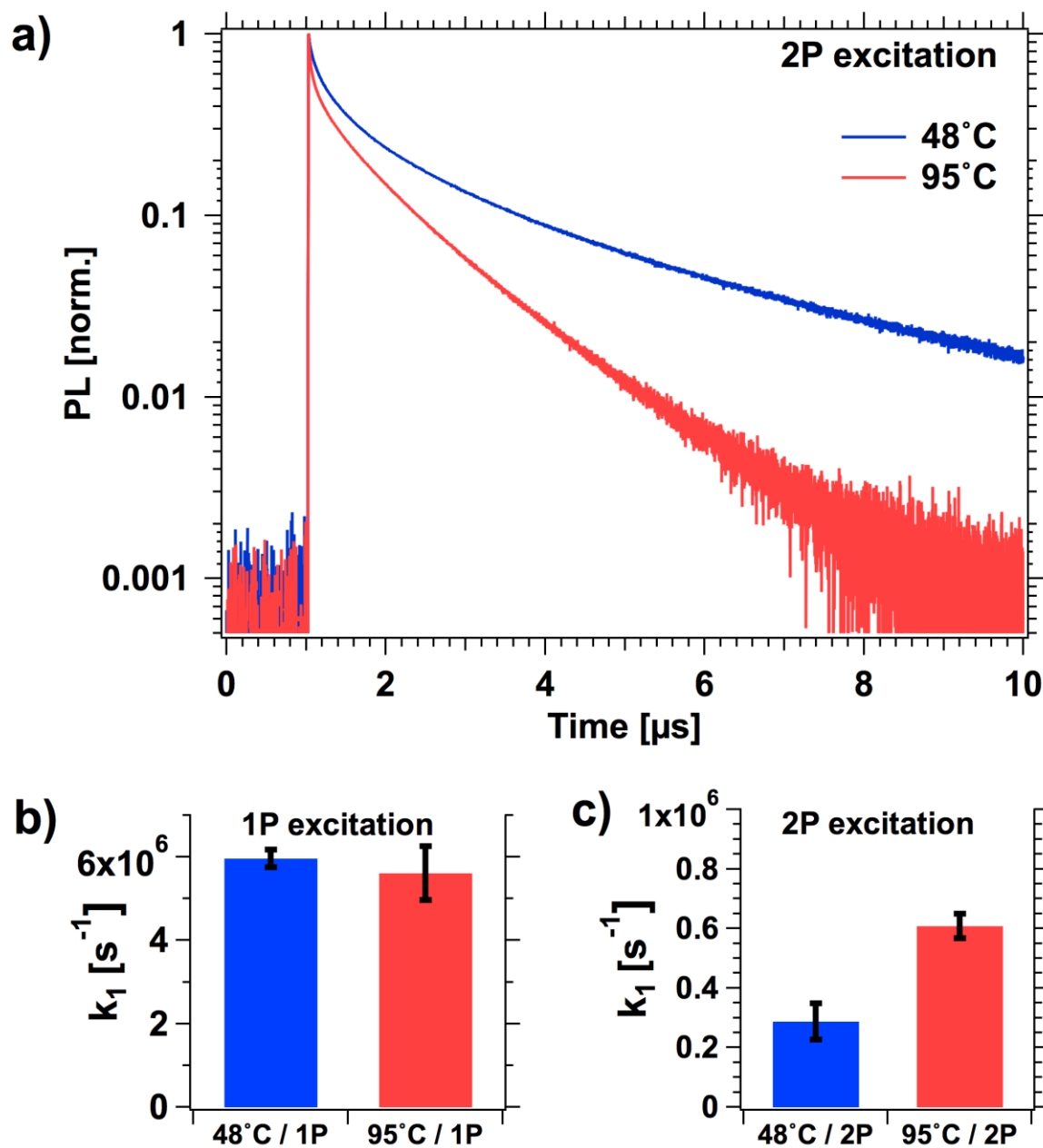


Figure 3: Photoluminescence of $\text{CH}_3\text{NH}_3\text{PbI}_3$ single crystals grown at 48°C (below the tetragonal to cubic phase transition) and at 95°C. a) 2-photon (2P) excitation PL transient ($\lambda_{\text{ex}} = 1400$ nm, fluence = 37 $\mu\text{J}/\text{cm}^2$); b) and c) first-order recombination coefficients for 1P and 2P excitation (averaged over 5 different excitation fluences).

In summary we have presented compelling evidence that the observed rapid crystallisation of metal halide perovskite crystals is due to the dissolution of colloids which can happen by a change in acidity of the solution, and due to a change in the solvent strength. The dissolved colloids increase the concentration of free ions in solution leading to supersaturation and the onset of crystallisation. Our findings opens a whole new depth of questions into understanding the interaction between solvent and colloids, which will catalyse further investigations. By direct addition of acid, we have demonstrated a much broader range of parameters including the temperature range and the solvent/salt combinations. By decoupling the temperature from the acidity, we have shown increased reaction yield, the growth of additional crystal systems and the growth of higher quality crystals with improved photoluminescence properties. High quality crystalline perovskites, in both large crystals and thin films, are at the core of the phenomenal optoelectronic properties of these materials. The thin film deposition is typically from the same solvents as used for the single crystal growth, and the same acid by-products will be present, at currently uncontrolled concentrations. Our work here will therefore have a direct impact upon researchers working on polycrystalline thin films, in addition to single crystals. The findings we report here are therefore of central importance to enabling the continued advancement of perovskite optoelectronics and to the improved reproducibility, homogeneity and eventual manufacturability of these technologies.

Acknowledgements: This work was funded by the EPSRC UK, the European Council Seventh Framework Programme (FP7) through the MESO project. PN and SN are supported by Marie Skłodowska-Curie actions individual fellowships (grant agreement number 653184 and 659306, respectively). DM is supported by the National Renewable Energy Laboratory Director's Fellowship, funded under DOE contract number DE-AC36-08GO28308. AAH is supported by EPSRC under Grant No. EP/M020517/1. KAV is supported by ERC-2010-StG-258600. OR and GR are funded by the Solar Photochemistry Program, Division of Chemical Sciences, Geosciences, and Biosciences, Office of Basic Energy Sciences, U.S. Department of Energy, under contract number DE-AC36-08GO28308 with the National Renewable Energy Laboratory. PK is supported by a European Research Council (ERC) starting grant (NanoScope). The authors thank Dr. M. Klug (Univ. Oxford) for his help in making the schematic figures.

Author contributions:

PN, DM, BW, NN and HJS discussed and planned the experiments required to understand the crystallization, including postulating the potential role of acids, as solvent degradation bi-products. PN synthesized the single crystals. DM performed the electrochemical measurements and prepared the iodide crystals at different temperature. BW performed the optical measurements. PN and BW performed the static light scattering measurements. SN and PN performed the FTIR measurements under the supervision of KV. AH performed the XRD measurements and analysis. AF performed the iSCAT measurement under the supervision of PK. OR performed the 1P-2P measurements under the supervision of GR. DM and NN prepared GHB and studied the degradation of solvents. PN and DM wrote the first draft of the manuscript and all the authors contributed to the writing of the final version of the manuscript. HJS supervised the project.

References

1. Stranks, S. D. & Snaith, H. J. Metal-halide perovskites for photovoltaic and light-emitting devices. *Nat. Nanotechnol.* **10**, 391–402 (2015).
2. Sessolo, M. & Bolink, H. J. Perovskite solar cells join the major league. *Science*. **350**, 917–917 (2015).
3. Yang, W. S. *et al.* High-performance photovoltaic perovskite layers fabricated through intramolecular exchange. *Science*. **348**, 1234–1237 (2015).
4. Berry, J. *et al.* Hybrid Organic-Inorganic Perovskites (HOIPs): Opportunities and Challenges. *Adv. Mater.* **27**, 5102–5112 (2015).
5. Wehrenfennig, C., Eperon, G. E., Johnston, M. B., Snaith, H. J. & Herz, L. M. High Charge Carrier Mobilities and Lifetimes in Organolead Trihalide Perovskites. *Adv. Mater.* **26**, 1584–1589 (2014).
6. Lin, Q. *et al.* Electro-optics of perovskite solar cells. *Nat. Photonics* **9**, 106–112 (2014).
7. Saidaminov, M. I. *et al.* High-quality bulk hybrid perovskite single crystals within minutes by inverse temperature crystallization. *Nat. Commun.* **6**, 7586 (2015).
8. Kadro, J. M., Nonomura, K., Gachet, D., Grätzel, M. & Hagfeldt, A. Facile route to freestanding CH₃NH₃PbI₃ crystals using inverse solubility. *Sci. Rep.* **5**, 11654 (2015).
9. Liu, Y. *et al.* Two-Inch-Sized Perovskite CH₃NH₃PbX₃ (X = Cl, Br, I) Crystals: Growth and Characterization. *Adv. Mater.* **27**, 5176–5183 (2015).
10. Dong, Q. *et al.* Electron-hole diffusion lengths 175 nm in solution-grown CH₃NH₃PbI₃ single crystals. *Science*. **347**, 967–970 (2015).

11. Nie, W. *et al.* High-efficiency solution-processed perovskite solar cells with millimeter-scale grains. *Science*. **347**, 522–525 (2015).
12. Zhang, T. *et al.* A facile solvothermal growth of single crystal mixed halide perovskite $\text{CH}_3\text{NH}_3\text{Pb}(\text{Br}_{1-x}\text{Cl}_x)_3$. *Chem. Commun.* **51**, 7820–7823 (2015).
13. Juillard, J. Dimethylformamide: purification, tests for purity and physical properties. *Pure Appl. Chem.* **49**, 885–892 (1977).
14. Munshi, T. *et al.* Monitoring of the interconversion of gamma-butyrolactone (GBL) to gamma hydroxybutyric acid (GHB) by Raman spectroscopy. *Drug Test. Anal.* **5**, 678–682 (2013).
15. Head, D. L. & Mccarty, C. G. The thermal decomposition of DMSO. *Tetrahedron Lett.* **14**, 1405–1408 (1973).
16. Zeroka, D. & Jensen, J. O. Infrared spectra of some isotopomers of methylamine and the methylammonium ion: a theoretical study. *J. Mol. Struct. THEOCHEM* **425**, 181–192 (1998).
17. Max, J.-J. & Chapados, C. Infrared Spectroscopy of Aqueous Carboxylic Acids: Comparison between Different Acids and Their Salts. *J. Phys. Chem. A* **108**, 3324–3337 (2004).
18. Zhou, Z. *et al.* Methylamine-Gas-Induced Defect-Healing Behavior of $\text{CH}_3\text{NH}_3\text{PbI}_3$ Thin Films for Perovskite Solar Cells. *Angew. Chemie Int. Ed.* **54**, 9705–9709 (2015).
19. Luan, M., Song, J., Wei, X., Chen, F. & Liu, J. Controllable growth of bulk cubic-phase $\text{CH}_3\text{NH}_3\text{PbI}_3$ single crystal with exciting room-temperature stability. *CrystEngComm* **18**, 5257–5261 (2016).
20. Johnston, M. B. & Herz, L. M. Hybrid Perovskites for Photovoltaics: Charge-Carrier Recombination, Diffusion, and Radiative Efficiencies. *Acc. Chem. Res.* **49**, 146–154 (2016).
21. Yamada, Y. *et al.* Dynamic Optical Properties of $\text{CH}_3\text{NH}_3\text{PbI}_3$ Single Crystals As Revealed by One- and Two-Photon Excited Photoluminescence Measurements. *J. Am. Chem. Soc.* **137**, 10456–10459 (2015).